5820–5836 *Nucleic Acids Research, 2016, Vol. 44, No. 12* *Published online 2 June 2016*
doi: 10.1093/nar/gkw499

Increased cytoplasmic *TARDBP* mRNA in affected spinal motor neurons in ALS caused by abnormal autoregulation of TDP-43

Akihide Koyama[1,2,†], Akihiro Sugai[1,†], Taisuke Kato[3,†], Tomohiko Ishihara[3], Atsushi Shiga[1,2], Yasuko Toyoshima[4], Misaki Koyama[1], Takuya Konno[1], Sachiko Hirokawa[3], Akio Yokoseki[3], Masatoyo Nishizawa[1], Akiyoshi Kakita[5], Hitoshi Takahashi[4] and Osamu Onodera[1,*]

[1]Department of Neurology, Clinical Neuroscience Branch, Brain Research Institute, 1-757 Asahimachi-dori, Chuo-ku, Niigata-City, Niigata 951-8585, Japan, [2]Center for Transdisciplinary Research, 1-757 Asahimachi-dori, Chuo-ku, Niigata-City, Niigata 951-8585, Japan, [3]Department of Molecular Neuroscience, Resource Branch for Brain Disease Research, Brain Research Institute, 1-757 Asahimachi-dori, Chuo-ku, Niigata-City, Niigata 951-8585, Japan, [4]Department of Pathology, Clinical Neuroscience Branch, Brain Research Institute, 1-757 Asahimachi-dori, Chuo-ku, Niigata-City, Niigata 951-8585, Japan and [5]Department of Pathology, Center for Bioresource-based Research, Brain Research Institute, Niigata University, 1-757 Asahimachi-dori, Chuo-ku, Niigata-City, Niigata 951-8585, Japan

Received November 8, 2015; Revised May 10, 2016; Accepted May 23, 2016

ABSTRACT

Amyotrophic lateral sclerosis (ALS) is a fatal motor neuron disorder. In motor neurons of ALS, TAR DNA binding protein-43 (TDP-43), a nuclear protein encoded by *TARDBP*, is absent from the nucleus and forms cytoplasmic inclusions. TDP-43 auto-regulates the amount by regulating the *TARDBP* mRNA, which has three polyadenylation signals (PASs) and three additional alternative introns within the last exon. However, it is still unclear how the autoregulatory mechanism works and how the status of autoregulation in ALS motor neurons without nuclear TDP-43 is. Here we show that TDP-43 inhibits the selection of the most proximal PAS and induces splicing of multiple alternative introns in *TARDBP* mRNA to decrease the amount of cytoplasmic *TARDBP* mRNA by nonsense-mediated mRNA decay. When TDP-43 is depleted, the *TARDBP* mRNA uses the most proximal PAS and is increased in the cytoplasm. Finally, we have demonstrated that in ALS motor neurons—especially neurons with mislocalized TDP-43—the amount of *TARDBP* mRNA is increased in the cytoplasm. Our observations indicate that nuclear TDP-43 contributes to the autoregulation and suggests that the absence of nuclear TDP-43 induces an abnormal autoregulation and increases the amount of *TARDBP* mRNA. The vicious cycle might accelerate the disease progression of ALS.

INTRODUCTION

In amyotrophic lateral sclerosis (ALS) and frontotemporal lobar degeneration, TAR DNA binding protein-43 (TDP-43), a nuclear RNA-binding protein, forms inclusion bodies in the cytoplasm and disappears from the nuclei of affected neurons and glial cells (1–4). The altered intracellular distribution of TDP-43 induces the alteration of TDP-43 function, which might underlie the molecular pathogenesis of ALS. Regulating its own amount is one of the functions of TDP-43 (5–8). Thus, it has been speculated that, in ALS, the mislocalization of TDP-43 influences the amount of TDP-43 through an autoregulatory mechanism (2,9). The homeostasis of the amount of TDP-43 is crucial for cell function and survival. Excess TDP-43 forms inclusion bodies, resulting in cell dysfunction and death in animal models (10–12), whereas a reduced amount of TDP-43 induces widespread dysregulation of mRNA metabolism in cultured cells and mouse brain (8,13–16). Two hypotheses have been proposed for the status of the TDP-43 autoregulation in ALS (2). If nuclear TDP-43 contributes to the autoregulation, loss of nuclear TDP-43 leads to increasing its biosynthesis and then TDP-43 accumulates, resulting in the formation of inclusion bodies. If cytoplasmic TDP-43 contributes to the autoregulation, ectopic cytoplasmic localization of TDP-43 decreases the TDP-43 synthesis and finally resulting in a disappearance of TDP-43 from the nucleus. However, it is not clear whether nuclear or cytoplasmic TDP-43 regulates the amount of TDP-43 (2). Moreover, it is unclear whether the the autoregulation of TDP-43 is preserved in the affected

*To whom correspondence should be addressed. Tel: +81 25 227 0684; Fax: +81 25 223 6646; Email: onodera@bri.niigata-u.ac.jp
†These authors contributed equally to the paper as first authors.

motor neurons with ALS. To resolve these issues, we have to elucidate the autoregulatory mechanism of TDP-43.

The autoregulation of TDP-43 is conducted by the *TARDBP* mRNA, which has three polyadenylation signals (PASs) (pA1, pA2 and pA4) and three additional alternative introns (intron 6, 7 and 8) within the last exon (Figure 1A and Supplementary Table S1) (5,6,8). For the downregulatory mechanism, two hypotheses have been proposed and still controversial whether a nonsense-mediated mRNA decay pathway contributes to the autoregulation (5–8). Using minigene and RT-PCR analysis, Polymenidou *et al.* have proposed that an isoform lacking introns 6 and 7 was degraded through a nonsense-mediated mRNA decay pathway (8). Meanwhile Baralle *et al*. have proposed that the spliceosomal assembly and/or constitutive processing of intron 7 lead to degradation of the *TARDBP* mRNA through an unknown mechanism (6,7). They have also proposed a mechanism that TDP-43 inhibits transport of *TARDBP* mRNA from the nucleus to the cytoplasm (7). Regarding the upregulatory mechanism of TDP-43, the mechanism has not been investigated, while it has been reported that mice with a half dose of the *TARDBP* gene, which encodes TDP-43, displayed normal levels of TDP-43 (17). Here we performed an in-depth analysis of the autoregulatory mechanism of TDP-43 with a focus on the upregulatory mechanism in response to TDP-43 depletion. Moreover, we investigated its autoregulatory status in ALS motor neurons without nuclear TDP-43.

MATERIALS AND METHODS

Plasmid construction

The full-length coding region of isoform I or isoform II of human TDP-43 cDNA (Figure 1E) was isolated from a human cDNA library (Clontech) and subcloned into a pcDNA DEST-40 vector (Invitrogen) (14,18). The original plasmid encoding the minigene was provided by Dr Hurng-Yi (National Taiwan University) (19). The wild-type exon 6 of TDP-43 and the enhanced-green fluorescence protein (EGFP)-fused minigene were amplified by polymerase chain reaction (PCR) with specific primers from the cDNA library and subcloned into the original minigene construct or the pEGFP-C3 vector (Clontech). The Δintron 6 or Δintron 7 minigene, AU-rich element mutant construct and spliced site mutant constructs were produced using the GeneArt site-directed mutagenesis system (Invitrogen). The primer sequences for construction of these plasmids are listed in Supplementary Table S2.

Cell culture, transfection, drugs and RNA interference

Full-length human TDP-43 coding regions tagged with myc were amplified by primers 5'-AAAGGA TCCATGTCTGAATATATTCGGGTA-3' and 5'-TTTCTCGAGCTACAGATCCTCTTCTGAGATGA GTTTTTGTTCCATTCCCCAGCCAGAAGACTT-3', followed by subcloning into the pcDNA5/FRT/TO vector and co-transfection into Flp-In T-REx™ HEK293 cells (Invitrogen) with Flp recombinase (encoding plasmid pOG-44). We cultured Flp-In T-REx™ HEK293, SH-SY5Y and HEK293T cells in Dulbecco's modified Eagle's medium (Gibco) supplemented with 10% fetal bovine serum. For Flp-In T-REx™ HEK293 selection, Hygromycin- and blasticidin-resistant colonies were pooled and expanded. Transgene expression was induced with 1 μg/ml doxycycline (Sigma). X-tremeGene HP DNA transfection reagent (Roche) was used for transfections. Cycloheximide (Sigma), actinomycin D (Sigma) and caffeine (Sigma) was used at a final concentration of 100 μg/ml, 5 μg/ml and 10 mM, respectively. Cells were transfected with small interfering RNA (siRNA) using Lipofectamine RNAi MAX (Invitrogen) according to the manufacturer's protocol. siRNA probes used in this study are summarized in Supplementary Table S2.

Western blot analysis

Cells were lysed with RIPA buffer (25 mM Tris–HCl, pH 7.6, 150 mM NaCl, 1% NP-40, 1% sodium deoxycholate and 0.1% sodium dodecyl sulphate) supplemented with protease inhibitor cocktail (Sigma) and centrifuged at 12,000 $\times g$ for 10 min at 4°C. The supernatant was resuspended in Laemmli Sample Buffer (BioRad). Anti-TDP-43 antibody (1:5000; Abnova), anti-TDP-43 (amino acids 3-12) antibody (for Figure 1I; 1:5000; Cosmobio), anti-Lamin B1 antibody (1:5000; MBL), anti-myc antibody (1:10,000; Millipore), anti-GFP antibody (1:5000; MBL), anti-DsRed polyclonal antibody (1:500; Clontech), anti-Actin antibody (1:5000; Santa Cruz) or anti-GAPDH antibody (1:10,000; MBL) was used as the primary antibody and subsequently detected with HRP-conjugated secondary antibodies (1:20,000; Dako). StartingBlock T20 blocking buffer (Thermo scientific) was used for Figure 1I.

In situ hybridization in *in vitro* cultured cells using the QuantiGene® ViewRNA technique

TARDBP mRNA was detected using the QuantiGene® ViewRNA ISH cell assay kit (Affymetrix) according to the manufacturer's instructions. TDP-43 tet-inducible Flp-In T-REx™ HEK293 cells were cultured on MAS-coated glass slides (MATSUNAMI glass) in the presence or absence of doxycycline for 48 h. Cells were fixed in 4% formaldehyde solution, permeabilized, treated with protease and hybridized with custom-designed QuantiGene® ViewRNA Type 4 (488 nm) probes targeting nucleotides 2055–2774 (probe set A) or nucleotides 373–1327 (probe set C) and Type 1 (550 nm) probes targeting nucleotides 2795–4198 (probe set B) of the human *TARDBP* mRNA (NM_007375). To visualize the hybridized probes, cells were incubated with pre-amplifier, amplifier and labeled probe. The cells were observed using a Zeiss LSM710 confocal laser-scanning microscope.

QuantiGene® ViewRNA *in situ* hybridization on formalin-fixed paraffin-embedded tissue

Supplementary Table S6 shows details of the patients and controls included in this study. For sporadic ALS (SALS) patients, the mutations in *TARDBP* and *SOD1* and G4C2 expansion in *C9ORF72* were excluded. This study was approved by the Institutional Ethical Review Board of Niigata University, written informed consent was obtained

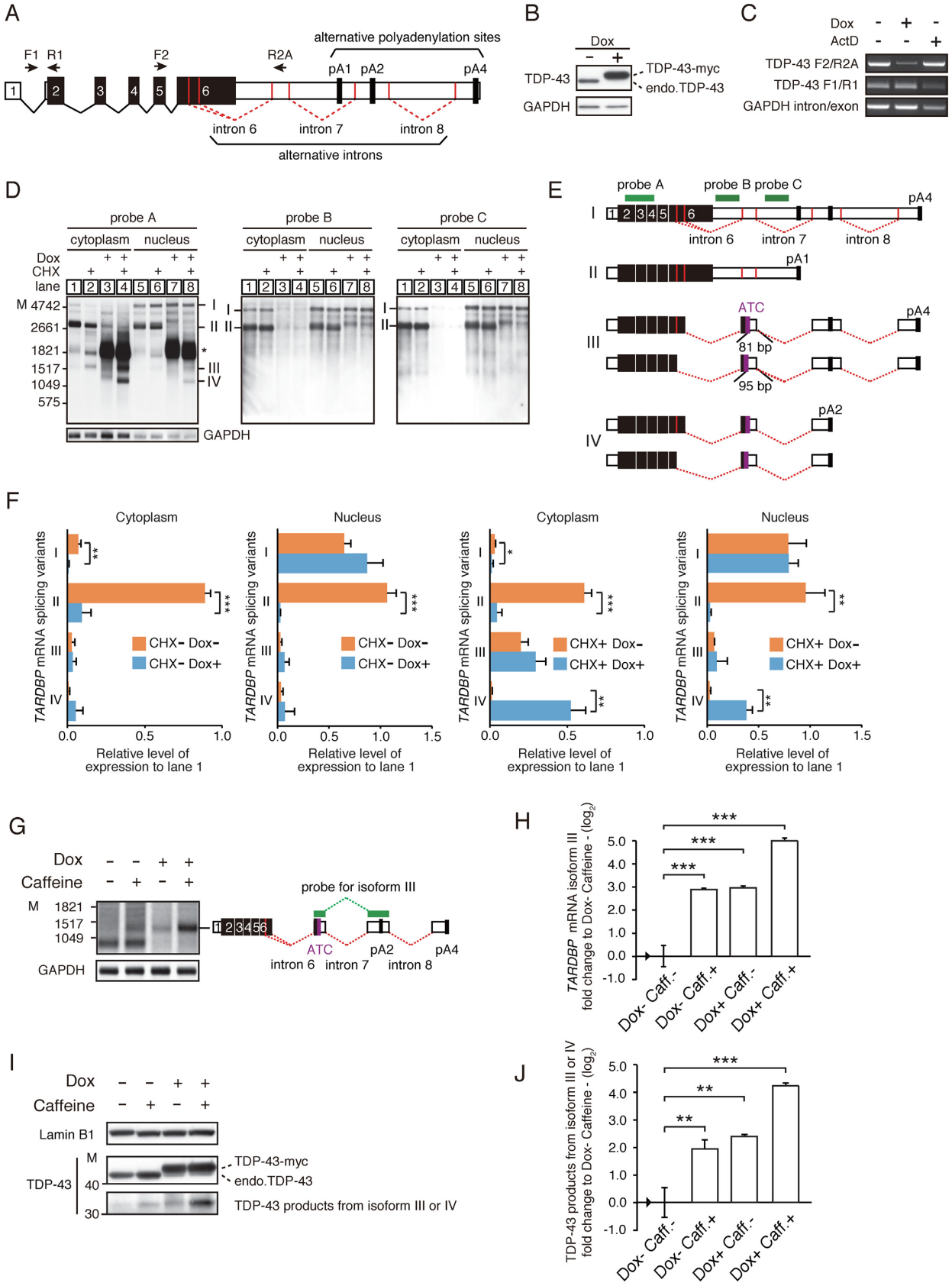

Figure 1. TDP-43 is downregulated via reduction in the amount of cytoplasmic *TARDBP* mRNA by nonsense-mediated mRNA decay. **(A)** Schematic representation of *TARDBP* mRNA and primers for RT-PCR. Black boxes represent the coding region. White boxes represent the non-coding region.

from the families and all clinical investigations were conducted according to the principles expressed in the Declaration of Helsinki. *In situ* hybridization was performed on a formalin-fixed paraffin-embedded 4-μm-thick lumbar section using a QuantiGene® ViewRNA ISH Tissue Assay kit (Affymetrix). Sections were fixed in 10% formaldehyde for 1 h, deparaffinized using Histoclear solution (National Diagnostics), boiled in pre-treatment solution (Affymetrix) for 20 min and digested with protease QF (Affymetrix) for 10 min. Sections were hybridized for 3 h at 40°C with custom-designed QuantiGene® ViewRNA Type 1 probes targeting nucleotides 373–1327 of human *TARDBP* mRNA (NM_007375; probe set C; Affymetrix) (Supplementary Figure S2A). Bound probes were then amplified using PreAmp1 QF and Amp1 QF molecules. Label Probe conjugated with alkaline phosphatase (Label Probe-AP) was then added, and Fast Red Substrate was used to produce signal. Slides were then counterstained with hematoxylin. Bright field and fluorescent microscopy images for each cell were taken by fluorescence microscopy (Keyence; BioRevo BZ-9000). We selected images of motor neurons in which a nucleolus was observable. The numbers of dot signals within the nucleus and the cytoplasm and the areas of the nucleus and cytoplasm were measured using Imaris software (Bitplane AG).

To examine the nuclear localization of TDP-43 and the intracellular distribution of *TARDBP* mRNA in the same cells, immunohistochemistry and *in situ* hybridization were performed using serial sections of spinal cord from SALS cases. For immunohistochemical analysis, heat retrieval using an autoclave for 10 min in 10 mM citrate buffer (pH 6.0) was applied to the sections. Immunofluorescence detection of TDP-43 was performed using a rabbit polyclonal antibody against TDP-43 (10782-2-AP, 1:3000; Proteintech). The secondary antibody used was Alexa Fluor 488 goat anti-rabbit IgG (1:300; Molecular Probes). The immunolabeled sections were counterstained with hematoxylin.

Cell fractionation and northern blot analysis

Cell fractionation was performed as described previously (20). Total RNA was extracted (Nucleospin RNAII; Takara Bio) and poly(A)$^+$ RNA was purified (NucleoTrap mRNA Mini kit; Takara Bio) according to the manufacturer's instructions. The RNA samples were loaded on 1.5% gels (NorthernMax-Gly Kit; Life Technologies), transferred to Hybond N+ nylon membranes (GE Healthcare) and probed with internally DIG-labeled sequences following pre-hybridization in ULTRAhyb hybridization buffer (Ambion). DIG-labeled RNA probes were prepared from template DNA amplified by specific primers (Supplementary Table S2) using a DIG Northern Starter Kit (Roche). Visualization of transcripts was performed with a CDP-Star reagent (Roche). Signals were detected by an LAS4000 mini biomolecular imager (GE Healthcare). The densitometric analysis of each band was performed by ImageQuant TL analysis software (GE Healthcare).

Quantitative real-time PCR

For cultured cells, first-strand cDNA was synthesized from total RNA by ReverTra Ace (TOYOBO) with random primers and an oligo(dT) primer (for standard qRT-PCR), or with P7-t25-vn primer (for 3′-end qRT-PCR) (21). For human materials, total RNA was extracted from frozen human spinal cords using the mirVana™ miRNA isolation kit (Ambion). Supplementary Table S5 shows details of the patients and controls included in this study. RNA quality was assessed based on the RNA integrity number, as determined using the Agilent 2100 Bioanalyzer (Agilent Technologies,). First-strand cDNA synthesis was performed using the SuperScript® VILO™ cDNA Synthesis Kit (Invitrogen). Informed consent was obtained from relatives prior to the study, and ethical approval was obtained from research ethics committees of Niigata University. qRT-PCR was performed with SYBR Green Premix ExTaq II on a TP-850 Real-Time PCR Detection system (Takara Bio) using a gene-specific primer pair (for standard qRT-PCR) or a gene-specific forward primer and P7 primer (for 3′-end

←

Vertical red lines indicate the splicing sites. The diagonal dashed red lines indicate the splicing. Intron 6 has three donor sites (nucleotide positions 769, 833 and 842 in cDNA). The 833 and 842 sites are represented as a single line. Bold black vertical lines indicate the polyadenylation signals (pA) (Supplementary Table S1). Arrows indicate primers (Supplementary Table S2). **(B)** Western blot analysis of Flp-In T-REx™ HEK293 cells with a TDP-43 complementary DNA with a myc sequence inserted into the FRT site with or without doxycycline (Dox) for 72 h using an anti-TDP-43 antibody. **(C)** RT-PCR analysis of endogenous *TARDBP* mRNA (amplified product between F2 and R2A) and endogenous *TARDBP* pre-mRNA (amplified product between F1 and R1). Samples treated with actinomycin D (ActD) (to halt transcription) were used as negative controls for amplification of endogenous *TARDBP* pre-mRNA. **(D)** Northern blot analysis of *TARDBP* mRNA. Poly (A)$^+$ RNA was extracted from the nuclear or cytoplasmic fraction in the absence or presence of Dox or cycloheximide (CHX) for 6 h. *Ectopic *TARDBP* mRNA. M indicates RNA size marker. Roman numerals correspond to those in (E). Hybridized with a probe for exons 2–4 (probe A); by a probe for intron 6 (probe B); and with a probe for intron 7 (probe C) (Supplementary Table S2). The lower panel hybridized with a probe for GAPDH. **(E)** Schematic representation of *TARDBP* mRNA isoforms and probes for northern blot analysis. Bold green lines represent probes. Vertical purple lines indicate the additional termination codons (ATCs). **(F)** Quantification of *TARDBP* mRNA isoforms by northern blot analysis using probe A. The roman numerals correspond to those in (E). Data represent the relative level of expression in lane 1. Orange bars correspond to samples without Dox. Blue bars correspond to samples with Dox. Data information: data are presented as mean ± SD ($n = 3$) *$P < 0.05$, **$P < 0.01$, ***$P < 0.001$, compared to Dox(−), *t*-test. **(G)** Northern blot analysis of *TARDBP* mRNA. Poly (A)$^+$ RNA was extracted from the cells treated with or without Dox or caffeine. Cells were cultured for 48 h in the presence of Dox. Next, cells were treated with caffeine for 24 h. The M indicates the RNA size marker. The lower panel was hybridized with a probe for GAPDH. Right panel: schematic representation of *TARDBP* mRNA isoform III and probes for northern blot analysis. The bold green line represents a probe for isoform III. Vertical purple lines indicate additional termination codons (ATCs). **(H)** The level of *TARDBP* mRNA isoforms lacking both intron 6 and intron 7 in the absence or presence of Dox or caffeine. **(I)** Western blot analysis of TDP-43 lacking both intron 6 and intron 7 in the absence or presence of Dox or caffeine with anti-Lamin B1 antibody (upper panel) and anti-TDP-43 antibody. M indicates protein size marker (kDa). **(J)** Quantitative analysis of TDP-43 products translated from isoform III or IV were normalized to the levels of lamin B1. They were then expressed as fold change relative to the sample in the absence of Dox and caffeine ($\log_2$) (mean ± SEM, $n = 3$) (black triangle: absence of Dox and caffeine). *$P < 0.05$, **$P < 0.01$, ***$P < 0.001$, multivariate two-way ANOVA followed by post hoc Bonferroni analysis.

qRT-PCR; Supplementary Table S2). PCR conditions were 30 s at 95°C for initial denaturing, followed by 40 cycles of 5 s at 95°C and 30 s at 60°C. Expression levels of the target gene relative to RPLP1 and RPLP2 were determined using the ΔΔCT method. Primer specificity was evaluated using the BLAST program (http://blast.ncbi.nlm.nih.gov/Blast.cgi), dissociation temperature measurements and agarose gel electrophoresis analysis. The sequences of primers are listed in Supplementary Table S2.

RNA-binding protein immunoprecipitation assay

Cell fractionation and native RIP were performed with the EZ-Magna Nuclear RIP™ (Native) Nuclear RNA-Binding Protein Immunoprecipitation Kit (Millipore) according to the manufacturer's instructions. Immunoprecipitation was performed using Dynabeads M-280 Sheep anti-Mouse IgG (catalog no. 11201D; Life Technologies), mouse anti-TDP-43 monoclonal antibodies (catalog no. 60019-2-Ig; Proteintech, or catalog no. H00023435-M01; Abnova) or mouse IgG (catalog no. CS200621; Millipore). The co-precipitated RNA were extracted with Nucleospin RNA XS (Takara Bio) and reverse-transcribed with SuperScript III (Invitrogen) using oligo(dT) primers. Synthesized cDNA was amplified with AmpliTaq Gold® 360 (Life Technologies) using specific primers (Supplementary Table S2).

RESULTS

TDP-43 induces *TARDBP* mRNA splicing variants susceptible to nonsense-mediated mRNA decay

To investigate the autoregulatory mechanism of TDP-43, we generated a stable Flp-In T-REx™ HEK293 cell line that contains a doxycycline-responsive transgene for the human TDP-43 complementary DNA (cDNA) coding region with a myc sequence. After 72 h of induction, expression of endogenous TDP-43 was completely suppressed (Figure 1B and Supplementary Figure S1A). RT-PCR analysis showed that the amount of *TARDBP* mRNA decreased (upper panel in Figure 1C), whereas the amount of pre-mRNA was not decreased (middle panel in Figure 1C), indicating that the transcriptional activity of *TARDBP* pre-mRNA is not affected. To investigate the alteration of endogenous *TARDBP* mRNA, including its intracellular distribution (5,7), we extracted poly(A)$^+$ RNA from nuclear and cytoplasmic fractions (Supplementary Figure S1B). We performed northern blot analysis using three probes: one for exons 2–4 (probe A) and two located in introns (intron 6 for probe B and intron 7 for probe C) (Figure 1D and E). The northern blot analysis and sequencing of the RT-PCR products revealed that intron 6 had three donor sites (nucleotide positions 769, 833 and 842 in cDNA); isoform III lacked introns 6, 7 and 8; and isoform IV lacked introns 6 and 7 (Figure 1E; Supplementary Figure S1C and D). Isoforms III and IV have additional termination codons located more than 55 bp upstream from the last exon–exon junction (Figure 1E). This condition fulfills the criteria for nonsense-mediated mRNA decay (8,22).

The isoform using pA1 was the most abundant product (isoform II in lanes 1 and 5 of Figure 1D), and the isoform using pA4 was the second most abundant product in the cytoplasm and the nucleus (I in lanes 1 and 5; Figure 1D). When TDP-43 was ectopically expressed, isoforms I and II of the endogenous *TARDBP* mRNA disappeared from the cytoplasm (Figure 1D and F). In the nucleus, isoform I showed no obvious change, whereas isoform II disappeared (Figure 1D and F). The results of RT-PCR analysis consistent with the results of northern blotting analysis (Supplementary Figure S1C and D). In addition, we have performed RT-PCR analysis in human neuroblastoma SH-SY5Y cells with transiently expressed TDP-43 (Supplementary Figure S1E and F). The results of RT-PCR analysis also consistent with the results obtained from Flp-In T-REx™ HEK293 cell (Supplementary Figure S1E and G).

Next, we investigated whether the cytoplasmic *TARDBP* mRNA was degraded by nonsense-mediated mRNA decay. We performed northern blot analysis in the presence of the nonsense-mediated mRNA decay inhibitor cycloheximide (CHX) (Figure 1D and F). With ectopic expression of TDP-43, the abundance of isoform IV was significantly increased in the cytoplasm (lane 4 in Figure 1D and F). By qRT-PCR analysis, we confirmed that the splicing isoform lacking both introns (not just intron 7) was more abundant in this condition (Supplementary Figure S2A and B). When UPF1, a central component of the nonsense-mediated mRNA decay pathway was depleted (Supplementary Figure S2C), the isoform lacking both introns was increased (Supplementary Figure S2D and E). Moreover, we treated the cells with caffeine which is a SMG1 kinase inhibitor and attenuate a nonsense-mediated mRNA decay by inhibiting the UPF1 phosphorylation cycle (23). The caffeine is more effective than UPF1 depletion on increasing in the isoform lacking both introns (Figure 1 G–I; Supplementary Figure S2F and G). Finally, under these conditions, we detected the product of truncated forms of TDP-43 thought to use additional termination codons, which are translated from nonsense-mediated mRNA decay sensitive mRNAs, isoforms III and IV (Figure 1J). Although the previous report discounted the contribution of a nonsense-mediated mRNA decay mechanism and emphasized that the splicing of intron 7 is enough for autoregulation (5,6,8), our analysis revealed the contribution of a nonsense-mediated mRNA decay mechanism for autoregulation and that both introns are spliced in the process.

In a northern blot analysis, we found that the amount of *TARDBP* mRNA using pA4 relative to that using pA1 was higher in the nucleus than in cytoplasm (I and II in Figure 1D and F). To investigate the intracellular distribution of *TARDBP* mRNA variants, we applied quantitative *in situ* RNA expression technology using QuantiGene® ViewRNA (Affymetrix). This method enabled us to quantitate the amount of mRNA by the number of spots (24). We performed a double *in situ* hybridization study using probes targeting intron 7 (probe set A) and pA2 to pA4 (probe set B) (Figure 2A). The spots that are positive for both probes indicate isoform I, and the spots that are only positive for probe set A indicate isoform II. The spots positive for probe set B were more abundant in the nucleus than the spots positive for probe set A (Dox-, Figure 2B), indicating that *TARDBP* mRNA using pA4 exists predominantly in the nucleus. This result was confirmed by a double *in situ* hybridization study using the probe set for exons 3–6 and

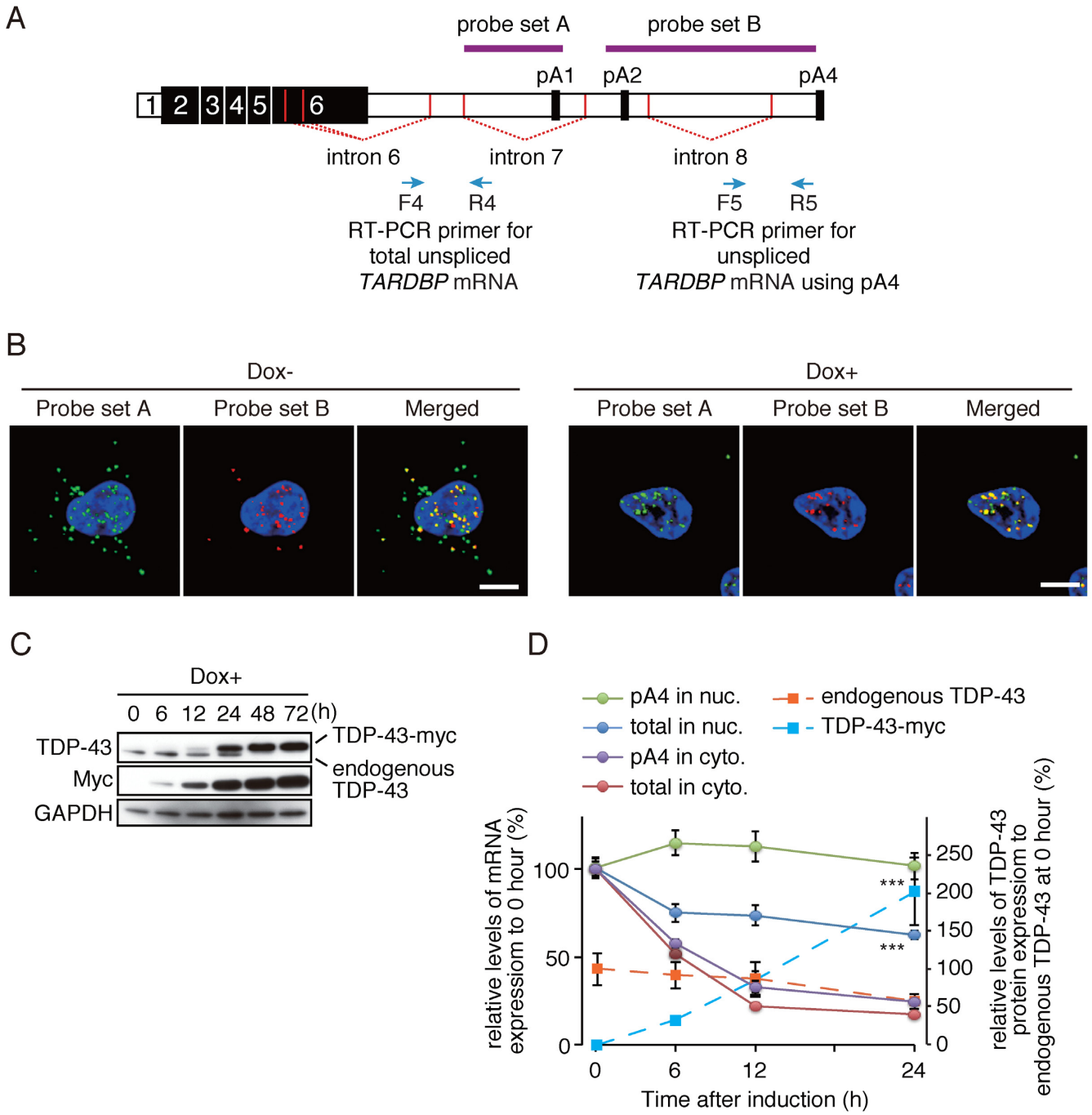

Figure 2. *TARDBP* mRNA using pA4 is relatively abundant and stable in the nucleus. (**A**) The location of the probe set of QuantiGene® ViewRNA for *in situ* hybridization and primers for quantitative RT-PCR analysis. Arrows indicate primers for qRT-PCR (Supplementary Table S2). Purple lines represent probes. (**B**) *In situ* hybridization with probe set A or B for TDP-43 tet-inducible Flp-In T-REx™ HEK293 cells in the absence (left panel) or presence (right panel) of doxycycline (Dox). *TARDBP* mRNA molecules with intron 7 are labeled green (probe set A: targeting nucleotides 2055–2774 [NM_007375]). *TARDBP* mRNA molecules with intron 8 are labeled red (probe set B: targeting nucleotides 2795–4198 [NM_007375]). The yellow spots in merged images have both introns. The nucleus is stained with Hoechst 33 342 (blue). Scale bar: 10 μm. (**C**) Time-course western blot analysis of TDP-43 after induction of ectopic TDP-43-myc by doxycycline (Dox). Anti-TDP-43 antibody (upper panel), anti-myc antibody (middle panel) and anti-GAPDH antibody (lower panel). (**D**) qRT-PCR time-course quantitative analysis of *TARDBP* mRNA and protein after induction of ectopic TDP-43-myc by doxycycline. Data (mean ± SD, $n = 6$) are expressed as relative to 0 h for mRNA (circle). Endogenous TDP-43 and TDP-43-myc protein are also quantified. Data (mean ± SEM, $n = 3$) are relative to the level of endogenous TDP-43 at 0 h (square). Cyto: in cytoplasm. Nuc: in nucleus. ***$P < 0.001$, multivariate two-way ANOVA followed by post hoc Bonferroni analysis for *TARDBP* mRNA.

probe set B (Supplementary Figure S3A and B). After 48 h of ectopic expression of TDP-43, *TARDBP* mRNA completely disappeared from the cytoplasm but not from the nucleus (Dox+, Figure 2B), as shown in northern blot analysis. Most of these spots in the nucleus were positive for both probe sets (merged panel in Figure 2B Dox+). We further investigated the levels of *TARDBP* mRNA isoforms at several time points after induction of ectopic TDP-43 expression. The ectopically expressed TDP-43 (TDP-43-myc) was detected at 6 h after induction, and a decrement in endogenous TDP-43 was observed at 24 h after induction (Figure 2C and D). The abundance of cytoplasmic *TARDBP* mRNA was markedly decreased at 6 h, whereas the abundance of the nuclear pA4 isoform was unchanged during the observed time points (Figure 2D).

TARDBP mRNA splicing after depletion of endogenous TDP-43

Next, to investigate the alteration of *TARDBP* mRNA in conditions of TDP-43 depletion, we used minigene constructs fused with exons from the survival of the motor neuron (*SMN*) gene and exon 6 of the human *TARDBP* gene (SMN-TDPwt) (Figure 3A). The transcripts derived from the minigene lack the Kozak consensus sequence and initiation codon. Therefore, a pioneer round translation, which is essential for nonsense-mediated mRNA decay, is not induced (25). By using this system, we were able to investigate the splicing variants in conditions free of nonsense-mediated mRNA decay and with depletion of the only endogenous *TARDBP* mRNA. We transfected the minigene into HEK293T cells under conditions of increased or decreased amount of TDP-43 (Figure 3B) and performed northern blot analysis using poly(A)$^+$ RNA from nuclear and cytoplasmic fractions (Figure 3C). The structures of each isoform were determined by sequencing of RT-PCR and 3′-RACE products (Figure 3D). Ectopic expression of TDP-43 resulted in decreased abundances of isoform II and increased abundances isoforms III and IV in the cytoplasm (Figure 3C, left panel, and E). In the nucleus, the abundance of isoform II was decreased, but the abundance of isoform IV was not significantly increased. These results were consistent with those observed with endogenous *TARDBP* mRNA, suggesting that the RNA metabolism of the minigene is similar to that of endogenous *TARDBP* mRNA. The depletion of endogenous TDP-43 increased the abundance of isoform II and decreased the abundances of isoforms III and IV in the cytoplasm (Figure 3C, right panel, and F). In the nucleus, the abundance of isoform II increased and the abundance of isoforms I and III decreased. The qRT-PCR analysis confirmed that the abundances of isoforms III and IV were increased by ectopic expression of TDP-43 and decreased by depletion of TDP-43 (Supplementary Figure S4A and B).

Splicing of intron 6 is important for autoregulation of TDP-43

Our results show that the splicing of introns 6 and 7 is regulated during the autoregulatory processes of TDP-43. We then investigated whether the splicing of intron 6 influences the amount of TDP-43. We used minigenes containing a part of exon 6 of the *TARDBP* fused with EGFP. The minigene uses the stop codon and PAS for the *TARDBP* gene (Figure 4A), allowing us to investigate the effect of 3′-UTR sequences of the *TARDBP* gene on the amount of EGFP fusion protein. To inhibit the splicing of the intron 6, we created substitutions of the nucleotide sequences at three donor sites and one acceptor site of intron 6 (m-intron 6) (Figure 4A). In this minigene, the splicing of intron 6 induced by ectopic expression of TDP-43 was inhibited (Figure 4B). The ectopic expression of TDP-43 reduces the abundance of EGFP fusion mRNA (Figure 4B and C) and protein (Figure 4D–F) in both minigenes. However, the reduction in the abundance of EGFP fusion mRNA and protein after ectopic expression of TDP-43 was significantly smaller with the m-intron 6 minigene than with the wild-type minigene (Figure 4C and F) indicating that splicing of intron 6 enhances the reduction in the abundance of the product.

Then, we investigated whether splicing of intron 7 is necessary for splicing of intron 6. First, we investigated the correlation between the splicing of introns 6 and 7 using minigenes lacking each intron (Supplementary Figure S5A). We found that TDP-43 efficiently induced the splicing of intron 7 in the minigene lacking intron 6 (Δintron 6a and b). In contrast, the splicing of intron 6 was not induced in the minigene lacking intron 7 (Δintron 7) (Supplementary Figure S5B). Next, we inhibited the splicing of intron 7 by substitution of the nucleotide sequences at the splicing donor site for intron 7 (Figure 4G). In this minigene, splicing of intron 6 was also inhibited (Figure 4H), indicating that splicing of intron 7 is essential for splicing of intron 6.

TDP-43 suppresses usage of the pA1 site

These results indicate that splicing of intron 7 is a primary event in the autoregulatory mechanism. For splicing of intron 7, which includes pA1, the usage of pA1 should be inhibited by TDP-43, as reported by Avendano-Vazquez *et al.* (5). To investigate this possibility, we compared the proportion of transcripts using pA1 and pA4 in whole unspliced isoforms upon expression or depletion of TDP-43 in cells transfected with SMN-TDP minigenes (Figure 3A). We selectively amplified the isoform using pA1 by using 3′-end qRT-PCR with a reverse primer targeting the polyadenylation site and a forward primer in intron 7 (Figure 5A) (21). The ectopic expression of TDP-43 markedly decreased the proportion of the isoform using pA1 and increased the proportion of the isoform using pA4 (Figure 5B, left panel). In contrast, the depletion of TDP-43 increased the proportion of the isoform using pA1 and decreased the proportion of the isoform using pA4 (Figure 5B, right panel). Next, to exclude the possibility that splicing of intron 7, in which pA1 exists, influence the selection of pA1, we inhibited the splicing of intron 7 by substituting the splicing site of intron 7 (Figures 4G and H; 5C). Because the 3′-end qRT-PCR method could not distinguish between isoforms using pA1 and those using pA2, we compared the proportion of isoforms extending beyond pA1 in whole unspliced isoforms upon expression or depletion of TDP-43. As expected, the ectopic expression of TDP-43 increased the pro-

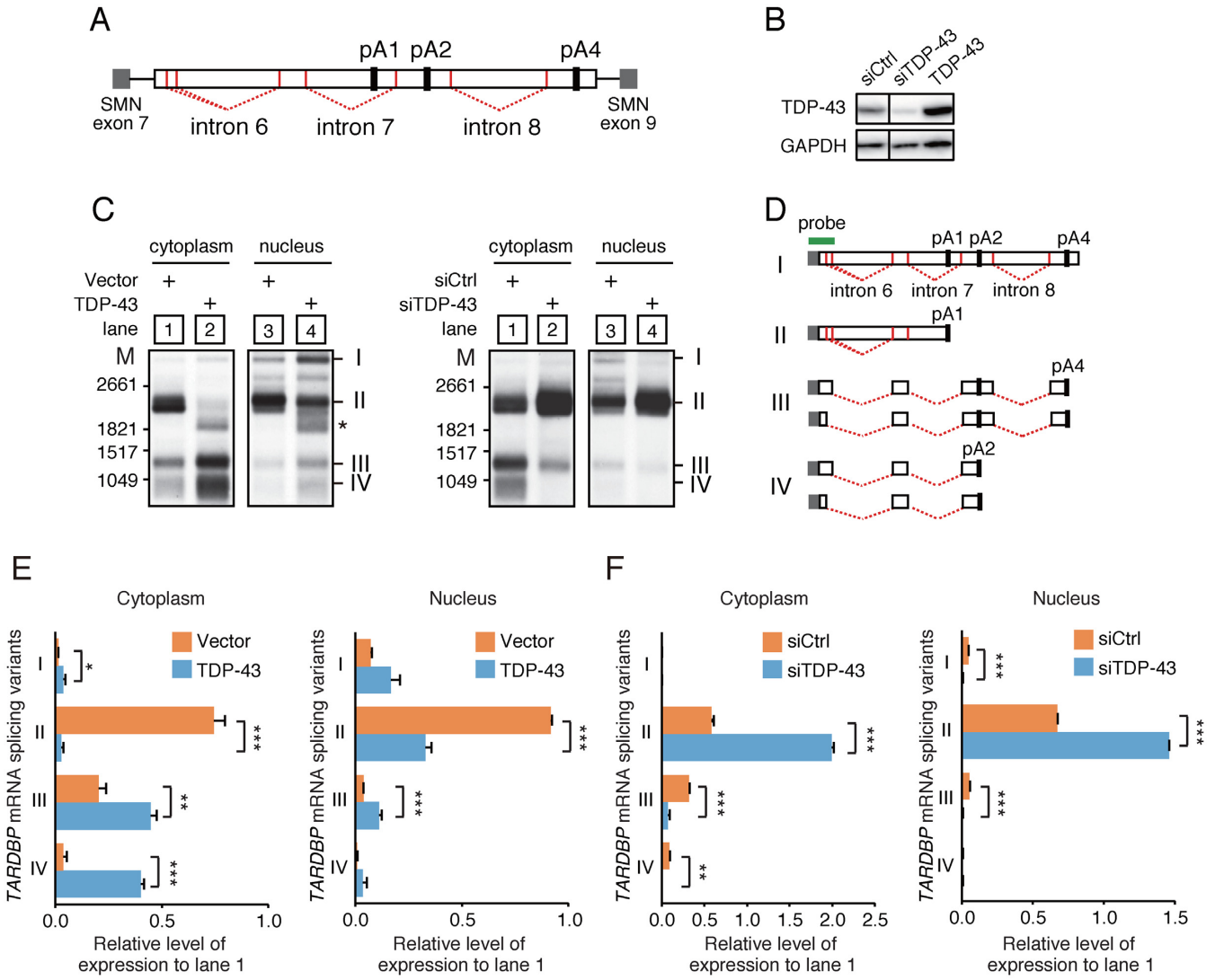

Figure 3. The depletion of TDP-43 inhibits splicing in exon 6 in the *TARDBP* gene. (**A**) Schematic representation of a minigene containing exon 6 of the human *TARDBP* gene. Gray boxes represent exons of the *SMN* gene. White boxes represent exon 6 of the human *TARDBP* gene. Vertical red lines indicate the splicing sites. Diagonal dashed red lines indicate the splicing between exons. Lines represent introns. Bold black vertical lines indicate the polyadenylation signals (pA). (**B**) Western blot analysis for TDP-43 in HEK293T cells co-transfected with control siRNA (siCtrl), TDP-43 siRNA (siTDP-43) or TDP-43 expression vector (probes are listed in Supplementary Table S2). (**C**) Northern blot analysis of poly(A)$^+$ RNA derived from the minigene. Poly(A)$^+$ RNA was extracted from the nuclear or cytoplasmic fraction from HEK293T cells transfected with the minigene (A). The results for cells co-transfected with TDP-43 cDNA plasmid or vector (left panel). The results for cells co-transfected with TDP-43 siRNA or control siRNA (right panel). *Ectopic *TARDBP* mRNA. M indicates RNA size marker. (**D**) Schematic representation of fusion minigene poly(A)$^+$ RNA isoforms and the probe for northern blot analysis. Gray boxes represent exon 7 of the *SMN* gene. White boxes represent exon 6 of the human *TARDBP* gene. Green line represents a probe. The diagonal dashed red lines indicate the splicing between exons in exon 6. pA indicates polyadenylation signal. (**E**) Quantification of minigene mRNA isoforms co-transfected with TDP-43 expression vector by northern blot analysis. (**F**) Quantification of minigene mRNA isoforms co-transfected with TDP-43 siRNA by northern blot analysis. Data information: the roman numerals in each graph correspond to those in (D). Data (mean ± SD, $n = 3$) represent values relative to the value in lane 1. *$P < 0.05$, **$P < 0.01$, ***$P < 0.001$, compared to vector or siCtrl lane in each variant by *t*-test.

portion of isoforms extending beyond pA1 (Figure 5D, left panel), whereas the depletion of TDP-43 decreased it, indicating that TDP-43 directly inhibits the usage of pA1 (Figure 5D, right panel).

The long 3′-UTR sequence of *TARDBP* mRNA does not alter its own stability

TDP-43 increased the abundance of mRNA using pA4 and decreased the abundance of cytoplasmic *TARDBP* mRNA. Because the 3′-UTR sequence contains a target sequence for miRNA or a putative adenylate uridylate-rich element that contributes to the stability of mRNA (25), the mRNA using pA4, which has a long 3′-UTR sequence, might be less stable than that using pA1. To explore this possibility, we compared the stability of mRNA using each PAS by halting mRNA transcription with actinomycin D in TDP-43 tet-inducible Flp-In T-REx^{TM} HEK293 cells. We found that the rates of degradation of *TARDBP* mRNA using pA4 were not significantly different from those of *TARDBP* mRNA using pA1, regardless of the presence or absence of doxycy-

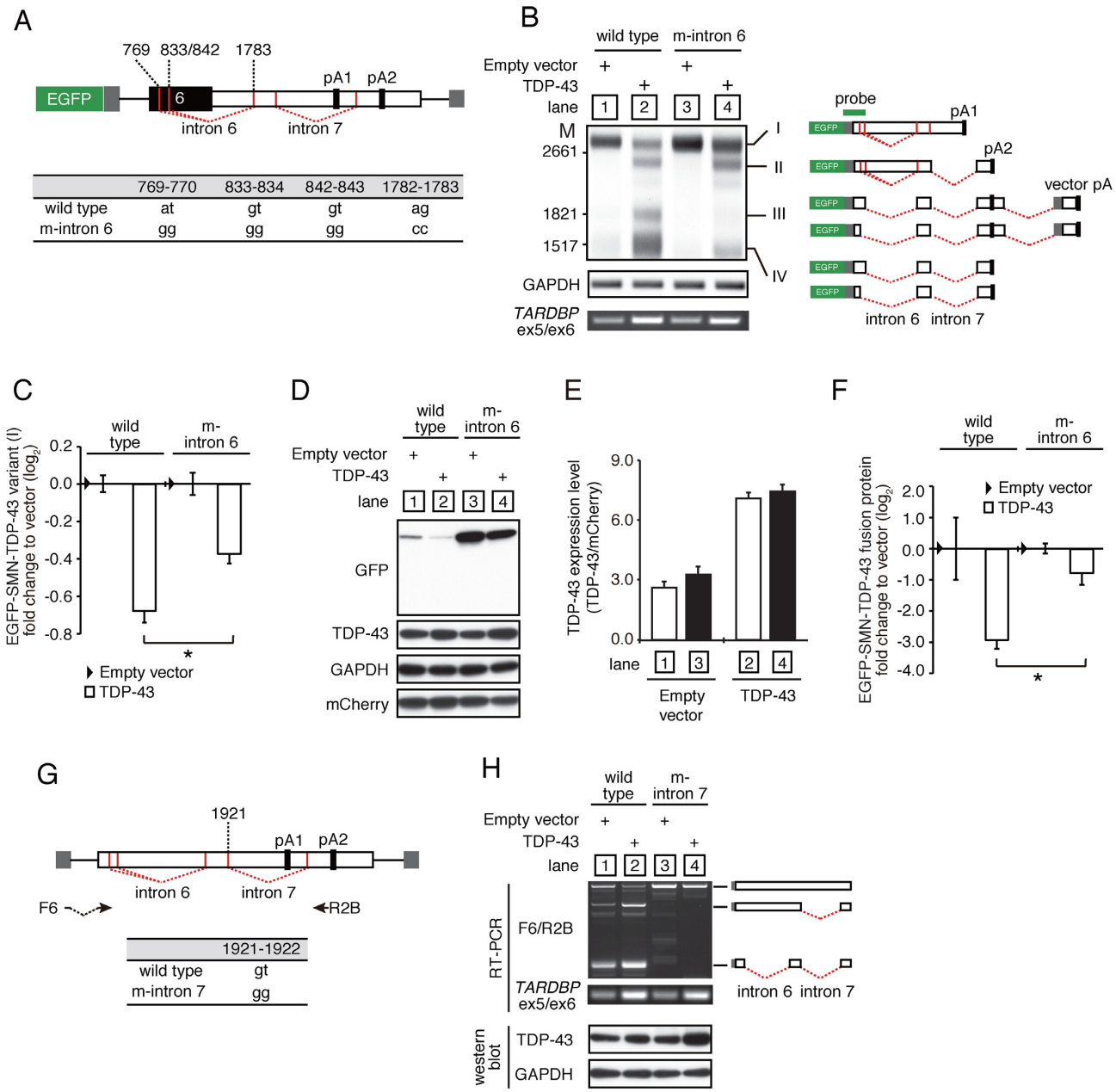

Figure 4. The significance of splicing intron 6. (**A**) Schematic representation of the EGFP-SMN-TDP-43 fused minigene and the location of the primers (primer sequences are listed in Supplementary Table S2). In m-intron 6, we substituted nucleotides at positions 769–770, 833–834 and 842–843 with guanine and at positions 1782–1783 with cytosine. Green box: EGFP; gray box: exons of the *SMN* gene; black box: coding region of exon 6; white box: non-coding region of exon 6; vertical red lines: splicing sites; diagonal lines: splicing between exons; arrows: primers; diagonal dashed lines within arrows: spanning exons; pA: polyadenylation signal. (**B**) Northern blot analysis of poly(A)$^+$ RNA derived from EGFP-fused minigene co-transfected with empty vector or TDP-43 cDNA in HEK293T cells (left upper panel). M indicates RNA size marker. The middle panel hybridized with a probe for GAPDH. The lower panel represents the *TARDBP* mRNA amplified by the primers between exon 5 (ex5) and exon 6 (ex6). The right panel represents the schematic representation of fusion minigene poly(A)$^+$ RNA isoforms and the probe for northern blot analysis. Gray boxes represent exon 7 of the *SMN* gene. The white boxes represent exon 6 of the human *TARDBP* gene, and the green line represents a probe. The diagonal dashed red lines indicate the splicing between exons in exon 6. pA indicates polyadenylation signal. (**C**) Quantitative analysis of EGFP-SMN-TDP-43 fusion poly(A)$^+$ RNA isoform I in (B). The levels of EGFP-SMN-TDP-43 fusion poly(A)$^+$ RNA isoform I were normalized to the levels of GAPDH, and then they were expressed as fold change relative to control (empty vector)($\log_2$) (mean ± SEM, $n = 3$) (black triangle: empty vector; white box: TDP-43 expression vector). *$P < 0.05$, *t*-test. (**D**) Western blot analysis with anti-GFP antibody, anti-TDP-43 antibody, anti-GAPDH antibody or anti-DsRed antibody for detection of mCherry. We co-transfected with the mCherry expression vector to adjust the transfection efficiency. (**E**) No difference in TDP-43 expression was observed between lanes 1 and 3 or lanes 2 and 4 in (D) (mean ± SEM, $n = 3$). (**F**) Quantitative analysis of EGFP-SMN-TDP-43 fusion proteins. The levels of EGFP-SMN-TDP-43 fusion proteins were normalized to the levels of mCherry, and then they were expressed as fold change relative to control ($\log_2$) (mean ± SEM, $n = 3$) (black triangle: empty vector; white box: TDP-43 expression vector). *$P < 0.05$, *t*-test. (**G**) Schematic representation of SMN-TDP-43 minigene with mutations at the spliced site of intron 7 and the location of the primers. We substituted nucleotides at positions 1921–1922 with guanine (m-intron 7). (**H**) RT-PCR analysis of RNA from HEK293T cells transfected with minigenes and either empty vector or the TDP-43 expression vector (upper left panel). The upper right panel represents the schematic representation for each product. Western blot analysis by anti-TDP-43 or anti-GAPDH antibody (lower panel).

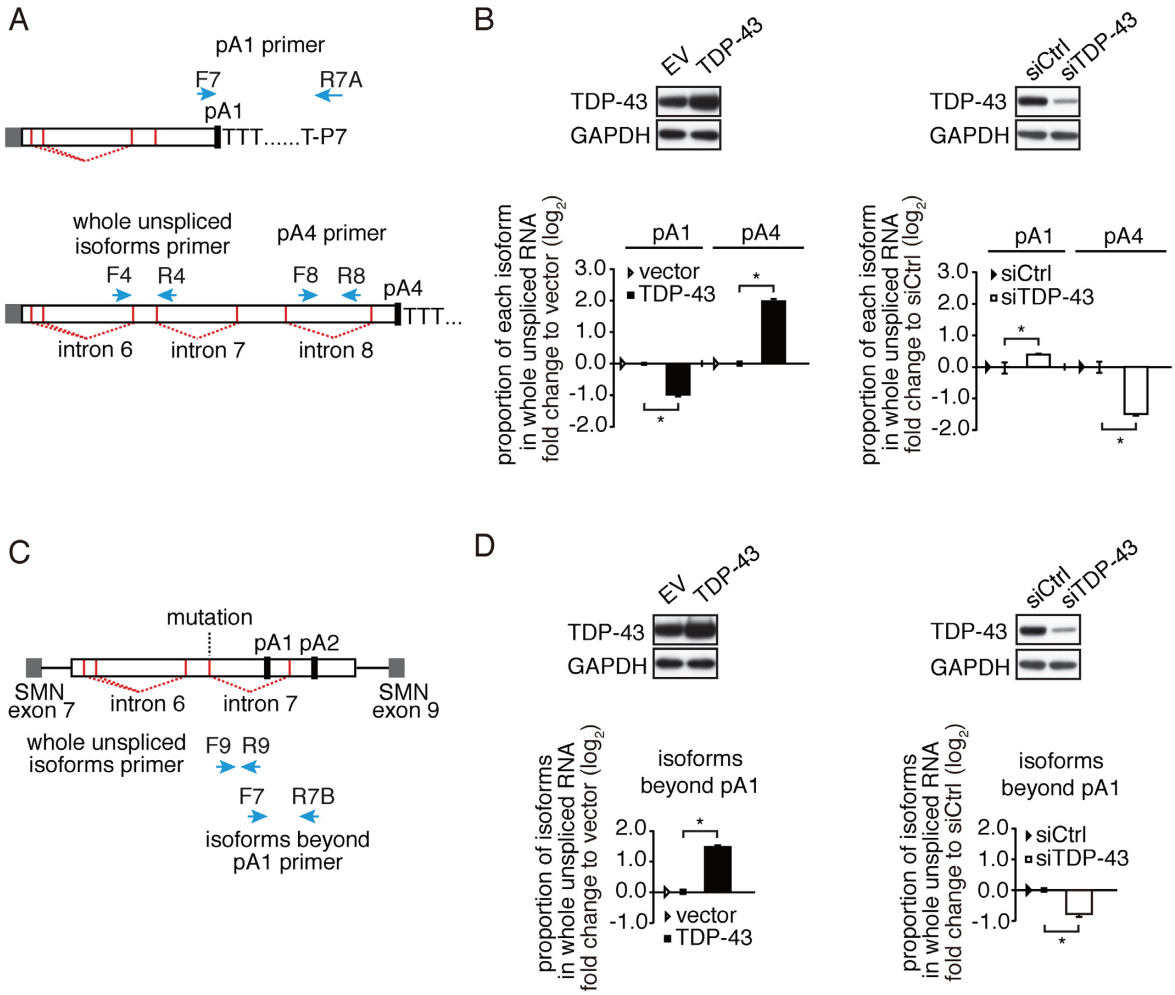

Figure 5. TDP-43 regulates the use of polyadenylation signals. (**A**) Schematic representation of cDNA derived from the minigene construct (Figure 3A) and the location of the primers. Gray boxes represent exons of the *SMN* gene. The arrows represent the primers. For analysis of the mRNA using pA1, we used P7-t25-vn primer first-strand cDNA synthesis (Supplementary Table S2) (21). (**B**) qRT-PCR analysis of fusion mRNA using each polyadenylation site with the minigene (Figure 3A) and TDP-43 plasmid (left panel) or TDP-43 siRNA (right panel) in HEK293T cells. Western blot analysis of TDP-43 expression (upper panel). Levels of each pA minigene isoform were measured by qRT-PCR and the relative values of whole unspliced isoforms were determined ($n = 3$) (lower panel). EV: empty vector; siCtrl: control siRNA. The probes are listed in Supplementary Table S2. (**C**) Schematic representation of the minigene with a mutation in the intron 7 donor site and the location of the primers for amplification. Gray boxes represent exons of the SMN gene. The arrows represent the primers (Supplementary Table S2). (**D**) qRT-PCR analysis of fusion mRNA from the minigene with a mutation at the intron 7 donor site (C) and TDP-43 plasmid (left panel) or TDP-43 siRNA (right panel) in HEK293T cells. Western blot analysis of TDP-43 expression (upper panel). Levels of isoforms containing sequences beyond pA1 were measured by qRT-PCR and the relative values of whole unspliced isoforms were determined (lower panel). TDP-43 EV: empty vector; siCtrl: control siRNA. The probes are listed in Supplementary Table S2. Data are expressed as fold-change relative to control ($\log_2$) and presented as mean ± SEM. Asterisks indicate statistically significant ($P < 0.05$, *t*-test) differences.

cline (Supplementary Figure S6A). We further investigated the effect of the putative adenylate uridylate-rich element by introducing nucleotide substitutions in this element (26); however, the stability of *TARDBP* mRNA was unchanged (Supplementary Figure S6B). These results indicate that the stability of *TARDBP* mRNA is not regulated by the 3′-UTR sequences.

The abundance of cytoplasmic *TARDBP* mRNA increases when TDP-43 is depleted

We found that a substantial amount of *TARDBP* mRNA exists in the nucleus. TDP-43 is a nuclear protein that binds to *TARDBP* mRNA via the TDP-43-binding region, which is located within intron 7 after the 3'-UTR sequence (6,8,15). Indeed, *TARDBP* mRNA using pA4 was co-isolated with TDP-43 from the nuclear fraction of HEK293T cells (Figure 6A). This result raises the possibility that depletion of TDP-43 facilitates the transport of *TARDBP* mRNA from the nucleus to the cytoplasm. By using northern blot analysis of poly(A)$^+$ RNA derived from HEK293T cells transfected with a SMN-TDP43-wt minigene, we found that TDP-43 depletion increased the amount of cytoplasmic mRNA using pA4 relative to that of cytoplasmic mRNA using pA1 (Figures 3C and F; 6B, left panel). The qRT-PCR assay also confirmed these results (Figure 6B, right panel). To investigate a possible role for the TDP-43-binding region, we compared the relative amount of cytoplasmic mRNA between the minigene lack-

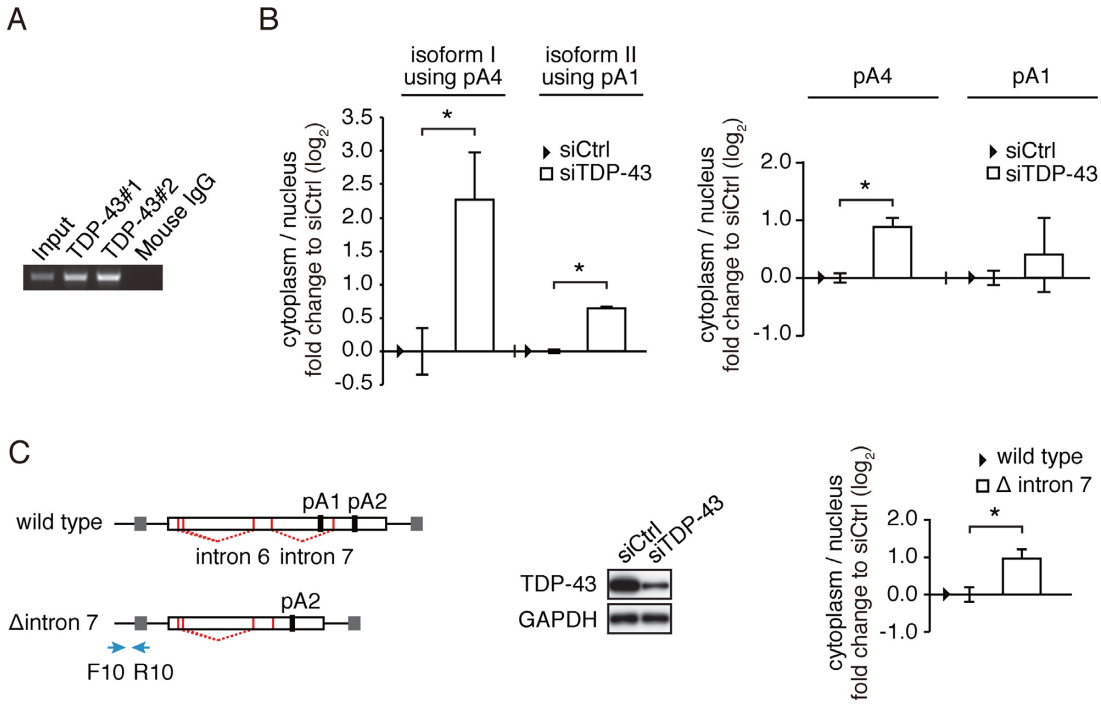

Figure 6. The amount of cytoplasmic *TARDBP* mRNA increases with depletion of TDP-43. (**A**) RT-PCR analysis of *TARDBP* mRNA co-immunoprecipitated with TDP-43 from the nuclear fraction of HEK293T cells. Amplified product using primers specific for transcripts using pA4: pA4 primer F and pA4 primer R (Supplementary Table S2). TDP-43#1: anti-TDP-43 antibody #1 (Abnova), TDP-43#2: anti-TDP-43 antibody #2 (Proteintech). (**B**) The cytoplasmic RNA-to-nuclear-RNA ratios of each isoform in HEK293T cells co-transfected with the minigene (see Figure 3A) and TDP-43 siRNA or control siRNA (siCtrl) ($n = 3$). Northern blot analysis of cytoplasmic RNA-to-nuclear-RNA ratio of isoforms I and II (left panel) (see Figure 3E). qRT-PCR analysis of minigene products, comparing isoforms using pA4 with those using pA1 (right panel)(see Figure 5A). Black triangle, siCtrl; white box, siTDP-43. (**C**) Cytoplasmic-to-nuclear ratio of minigene RNA in HEK293T cells transfected with a Δintron 7 minigene was compared to that of cells transfected with a wild-type minigene by qRT-PCR ($n = 3$). Schematic representation of minigenes (left panel). The arrows represent the primers. Western blot analysis of TDP-43 expression in HEK293T cells co-transfected with control siRNA (siCtrl) or TDP-43 siRNA (siTDP-43) (middle panel). Comparison of cytoplasmic-to-nuclear ratio of minigene RNA between wild-type and Δintron 7 minigene transfected cells (right panel). Data information: data are expressed as fold change relative to control ($\log_2$) and presented as mean ± SEM. Asterisks indicate statistically significant ($P < 0.05$, *t*-test) differences. Primer sequences are listed in Supplementary Table S2.

ing the TDP-43-binding region (Δintron 7) and that of wild-type cytoplasmic mRNA (Figure 6C, left panel). The cytoplasmic-to-nuclear ratio of RNA was higher in mRNA lacking the TDP-43-binding region (Figure 6C, middle and right panel).

Abundances of cytoplasmic and total *TARDBP* mRNA are increased in ALS spinal motor neurons

Although TDP-43 loses the nuclear localization in affected neurons in ALS, the autoregulatory status of TDP-43 in these neurons have not been investigated. We then addressed this issue using postmortem spinal cord tissue from ALS patients. At first, we investigated the expression level of total *TARDBP* mRNA and *TARDBP* mRNA lacking both intron 6 and intron 7 in RNAs obtained from spinal cords of SALS or control. Although the amount of *TARDBP* mRNA lacking both intron 6 and intron 7 decreased in ALS as expected, the amount of total *TARDBP* mRNA did not increase as previously reported (Figure 7A and B) (27).

Our data indicate that a depletion of nuclear TDP-43 increases cytoplasmic *TARDBP* mRNA, which should be translated into TDP-43 and decreases the nuclear *TARDBP* mRNA. This system does not just increase the total amount of mRNA, but redistributes the mRNA to increase the mRNA translated into the protein. Moreover, the number, size and status of neurons may influence the amount of the mRNA. Therefore, we attempted to investigate whether the cytoplasmic—and not nuclear—*TARDBP* mRNAs was increased in each spinal motor neurons. Thus, we applied quantitative *in situ* hybridization technology using QuantiGene® ViewRNA. We counted the number of spots for *TARDBP* mRNA in the nucleus and cytoplasm of spinal motor neurons from control, SALS and familial ALS patients (Figure 7A and C) (24). Familial ALS patients included ALS1 (caused by a mutation in the *SOD1* gene and shows no TDP-43 pathology) and ALS10 (caused by a mutation in the *TARDBP* gene and shows TDP-43 pathology) patients (4,18,28,29).

The *TARDBP* mRNA spots were observed in the nucleus and cytoplasm of spinal motor neurons (Figure 7C and Supplementary Figure S7). The mean number of *TARDBP* mRNA spots in neurons from SALS patients decreased in the nucleus and increased in the cytoplasm compared to controls; however, the differences were not significant (Supplementary Figure S7). Because cell size is positively associated with the amount of *TARDBP* mRNA (Supplementary Table S4), and because it has been reported that cell size is smaller in SALS than in control neurons (30), we

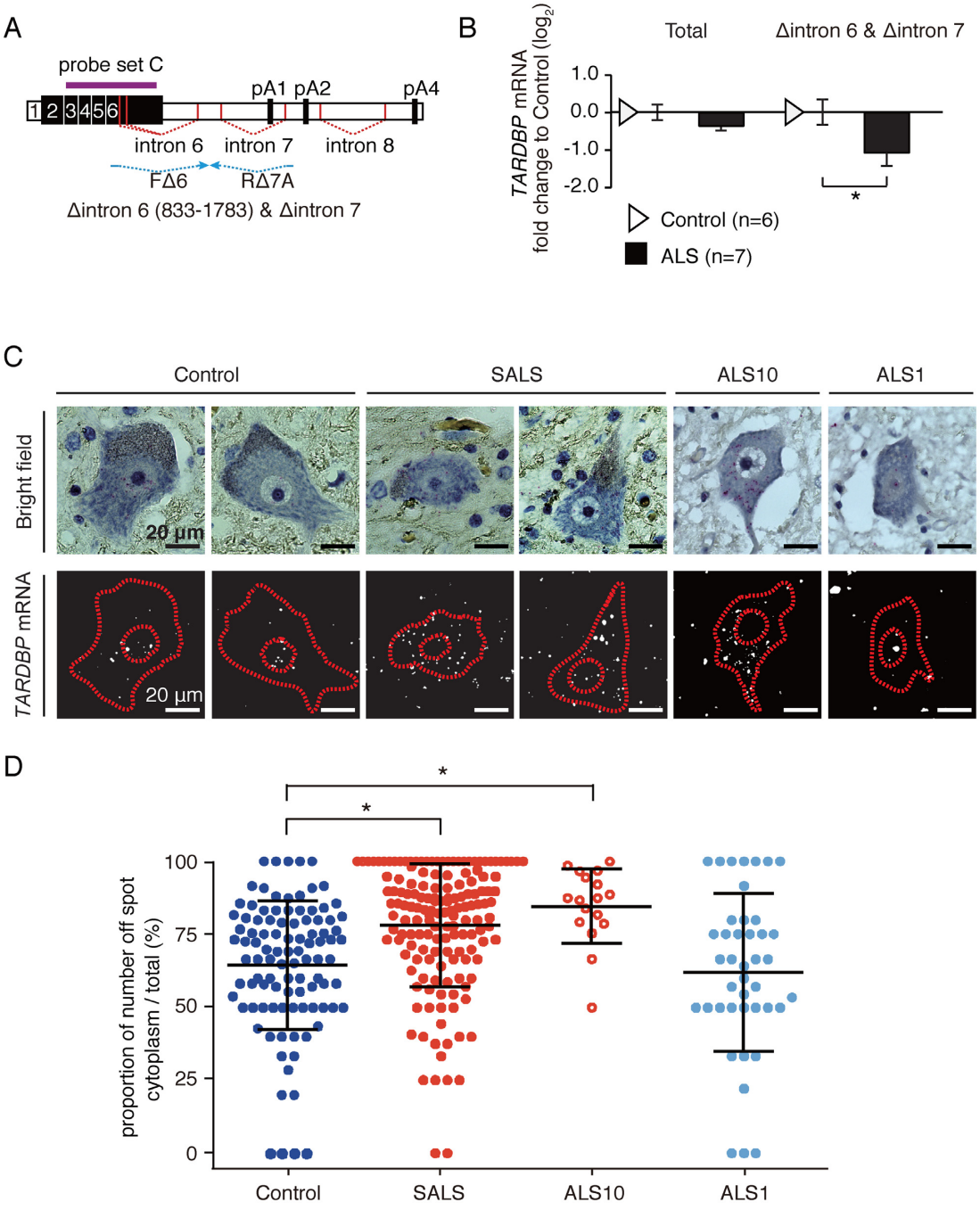

Figure 7. Alteration of *TARDBP* mRNA intracellular distribution in spinal cord motor neurons of ALS. (**A**) Schematic representation of *TARDBP* mRNA and primers for RT-PCR (blue arrows) and the location of the probes for *in situ* hybridization (bold purple line). Black boxes represent the coding region. White boxes represent the noncoding region. Vertical red lines indicate the splicing sites. The diagonal dashed red lines indicate the splicing. (**B**) Quantitative RT-PCR analysis of TDP-43 mRNA in spinal cord with ALS or control. The expression level was normalized by the expression level of RPLP1. Data are expressed as fold change relative to control ($\log_2$) and presented as mean ± SEM. Asterisks indicate statistically significant ($P < 0.05$, *t*-test) differences. Supplementary Table S5 shows details of the patients and controls included in this study. (**C**) Quantitative *in situ* hybridization for the spinal motor neurons from lumbar spinal cord of controls, SALS cases, a familial ALS case carrying a mutation in *TARDBP* (ALS10: p.Gln343Arg) (18) and familial ALS cases carrying mutations in *SOD-1* (ALS1: p.Asp101Tyr and p.Ala4Thr) (4,28,29). Supplementary Table S6 shows details of the patients and controls included in this study. Upper panels: bright field image of hematoxylin staining. Lower panels: *in situ* hybridization detection for *TARDBP* mRNA (white). Red dashed lines represent outlines of the displayed motor neurons and its nucleus. Scale bar, 20 μm. (**D**) Scatter gram of the proportion of the cytoplasmic *TARDBP* mRNA in the examined spinal motor neurons. The lines and error bars represent the mean ± SD. Asterisks indicate statistically significant differences ($P < 0.01$, Steel-Dwass non-parametric multiple comparison test following Kruskal-Wallis non-parametric ANOVA).

investigated the proportion of *TARDBP* mRNA in the cytoplasm. The proportion of *TARDBP* mRNA in the cytoplasm showed a Gaussian distribution in the controls; however, in SALS neurons, the distribution of the proportion was markedly shifted to 100 (Figure 7D and Supplementary Table S3). The mean values of the proportion of cytoplasmic *TARDBP* mRNA in SALS and ALS10 were significantly larger, by 121 and 131%, respectively, than those in controls. In contrast, the mean values of the proportion of cytoplasmic *TARDBP* mRNA in ALS1 were similar to those in controls. We performed a stepwise multiple linear regression analysis using cell size and ALS status (control or SALS) as independent variables (Table 1). The status of SALS was selected as a negative factor for the number of nuclear *TARDBP* mRNA spots and a positive factor for the number of cytoplasmic or total *TARDBP* mRNA spots.

Finally, we compared the number of *TARDBP* mRNA spots between neurons with nuclear TDP-43 (unaffected neurons) and those with cytoplasmic TDP-43 inclusions (affected neurons) in SALS (Figure 8A). The *TARDBP* mRNA spots did not co-localize with cytoplasmic TDP-43 inclusions (Figure 8A, bottom panel). The number of *TARDBP* mRNA spots was not significantly different between affected neurons and unaffected neurons (Figure 8B). The mean value of the proportion of cytoplasmic *TARDBP* mRNA in affected neurons was significantly larger, by 134%, than in unaffected neurons (Figure 8C).

DISCUSSION

We demonstrated the autoregulatory mechanism of TDP-43 under conditions of increased or depleted TDP-43 by northern blot analysis of endogenous *TARDBP* mRNA and using a minigene reporter assay. A model for the autoregulatory mechanism of TDP-43 is proposed in Figure 9A. Autoregulation is performed by the coordination of selection of the polyadenylation signal and alternative splicing accompanied by regulation of intracellular distribution of *TARDBP* mRNA. In conditions of excess nuclear TDP-43, TDP-43 inhibits the selection of pA1 by binding to intron 7 of *TARDBP* pre-mRNA (5), resulting in elongation of transcripts beyond pA1. The elongated transcripts present the acceptor site of intron 7. Then, the transcript undergoes intron 7 splicing, followed by intron 6 splicing. The isoform is exported to the cytoplasm and degraded by nonsense-mediated mRNA decay (8), resulting in a decrement in the cytoplasmic *TARDBP* mRNA. Some transcripts that escape intron 7 splicing select pA4. The mRNA molecules that use pA4 tend to be retained in the nucleus with nuclear TDP-43 through the binding of TDP-43 to the 3'-UTR sequence beyond pA1 (5,8,15). When nuclear TDP-43 is depleted, *TARDBP* transcripts select pA1 and are transported to the cytoplasm, resulting in an increase in the amount of cytoplasmic *TARDBP* mRNA.

Two hypotheses have been proposed to explain how the autoregulatory mechanism of TDP-43 contributes to the molecular pathogenesis of ALS (2). These hypotheses differ as to whether nuclear or cytoplasmic TDP-43 contributes to the autoregulation. Our results from cultured cells indicate that the amount of TDP-43 is regulated by the amount of cytoplasmic *TARDBP* mRNA. In ALS, the nuclear TDP-43 decreases and cytoplasmic TDP-43 increases as inclusions. Thus, if nuclear TDP-43 contributes to the autoregulation, then the amount of cytoplasmic *TARDBP* mRNA increases. On the contrary, if cytoplasmic TDP-43 contributes to the autoregulation, then the amount of cytoplasmic *TARDBP* mRNA decreases. We found that the amount of cytoplasmic *TARDBP* mRNA increased in affected neurons from SALS patients, indicating that nuclear TDP-43 contributes to the autoregulation. An increased amount of cytoplasmic *TARDBP* mRNA may lead to an increase in TDP-43 in affected neurons in ALS. If the newly synthesized TDP-43 is recruited into cytoplasmic inclusions, then nuclear TDP-43 is consistently depleted. The continued depletion of nuclear TDP-43 in ALS would continuously upregulate the synthesis of TDP-43. This would be a vicious cycle that may accelerate the disease progression in ALS proposed by Lee *et al.* (2).

The quantification of the amount of mRNA in a single cell is challenging. The previous analysis using a microarray assay did not show a difference of *TARDBP* mRNA in spinal motor neurons between ALS and control samples (27). The difference between the previous result and ours might be due to the microarray analysis not being sensitive enough to detect the alteration of the amount of *TARDBP* mRNA and/or to the fact that the size of the neurons was not considered in the previous report. We applied quantitative *in situ* hybridization technology using QuantiGene® ViewRNA to investigate the amount and intracellular distribution on mRNA in the human spinal motor neurons (24). The result for ALS1, in which the amount of cytoplasmic *TARDBP* mRNA did not change, further confirmed that the findings are not simply a result of dysfunction of spinal motor neurons.

Regarding the downregulatory mechanism of TDP-43, our results confirmed the hypothesis proposed by Polymenidou *et al.,* which is that the splicing of introns 6 and 7 leads to degradation of mRNA through a nonsense-mediated mRNA decay mechanism (8). Although they proposed the hypothesis based on the result of an RT-PCR analysis of minigene-derived RNA (8), we demonstrated by northern blot analysis that the endogenous mRNA transcripts were susceptible to nonsense-mediated mRNA decay. The autoregulatory mechanism of alternative splicing associated with nonsense-mediated mRNA decay has been reported in RNA-binding proteins (31,32). These proteins have several characteristic features in their last exon: 1) large size; 2) a nucleotide sequence that is highly conserved among species; and 3) amino acid sequences that have been predicted to have a disordered structure (31,33). TDP-43 is an RNA-binding protein, and the last exon of the *TARDBP* gene has these characteristic features (34).

Baralle *et al*. have reported that the transcripts susceptible to nonsense-mediated mRNA decay were not observed by northern blot analysis. Thus they have disagreed about the contribution of mRNA transcripts lacking intron 6 and of nonsense-mediated mRNA decay (6). However, we were able to find the transcripts susceptible to nonsense-mediated mRNA decay by northern blot analysis for several reasons. First, we used *TARDBP* exons 2–4 for the probe in the northern blot analysis, whereas Baralle's group used intron 7 or a unique fragment lacking both introns 6 and 7 (6).

Table 1. Multiple regression analysis of *TARDBP* mRNA and neuron compartment

	Standardized regression coefficient		Coefficient of determination (adjusted r^2)
	SALS	Neuron area (μm^2)	
Nuclear *TARDBP* mRNA	−1.026*	0.001**	0.096**
Cytoplasmic *TARDBP* mRNA	3.937*	0.006**	0.208**
Total *TARDBP* mRNA	2.911*	0.007**	0.199**

We performed a stepwise multiple linear regression analysis using the neuron compartment and SALS (sporadic ALS) as independent variables to examine the independent predictors of the number of *TARDBP* mRNA spots. Correlation coefficients are shown. *$P < 0.05$, **$P < 0.01$.

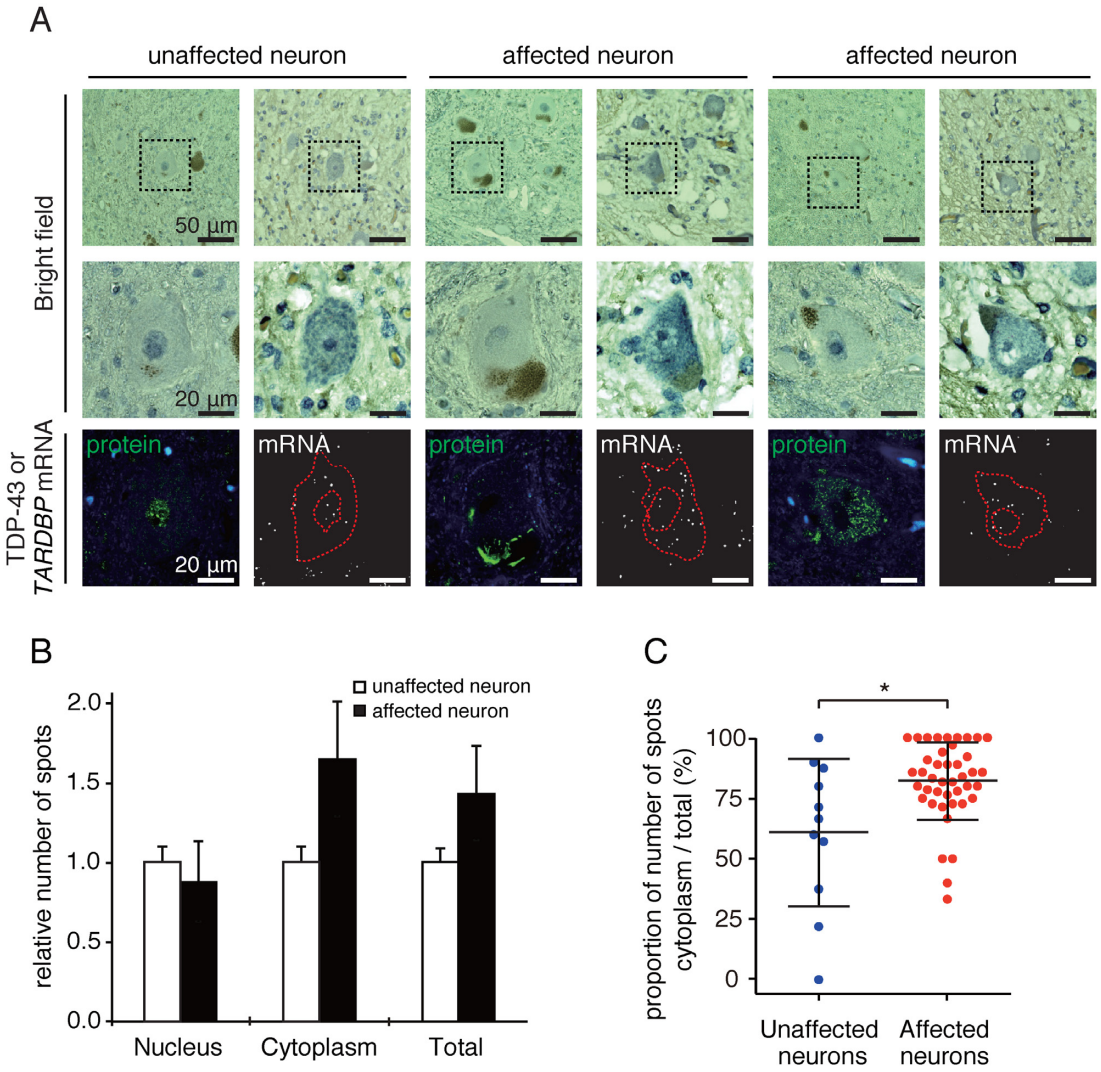

Figure 8. Alteration of *TARDBP* mRNA intracellular distribution in motor neurons with TDP-43 cytoplasmic inclusions. (**A**) Quantitative *in situ* hybridization for SALS spinal motor neurons in the presence (SALS: unaffected neurons) or absence of nuclear TDP-43 (SALS: affected neurons). Shown are representative motor neurons from lumbar spinal cord serial sections from patients with sporadic ALS (SALS) labeled with QuantiGene® ViewRNA probe for *TARDBP* mRNA or immunostained with TDP-43 antibody and counterstained with hematoxylin. Upper panels: lower magnification images of motor neurons displayed in middle panels. Scale bar, 50 μm. Black dashed squares depict location of the motor neurons. Middle panels: bright field images of hematoxylin staining for the spinal motor neurons from the SALS subjects. Lower panels: immunostaining with anti-TDP-43 antibody (green) and *in situ* hybridization detection for *TARDBP* mRNA (white). Red dashed lines represent outlines of the displayed motor neurons and the nucleus. Scale bar, 20 μm. (**B**) Number of spots for nuclear, cytoplasmic and total *TARDBP* mRNA from affected ($n = 42$) or unaffected ($n = 11$) spinal motor neurons. The lines and error bars represent the mean ± SEM. (**C**) Scatter gram of the proportion of cytoplasmic *TARDBP* mRNA in the examined spinal motor neurons of ALS patients. The lines and error bars represent the mean ± SD. Asterisks indicate statistically significant ($P < 0.05$, Mann–Whitney U test) differences.

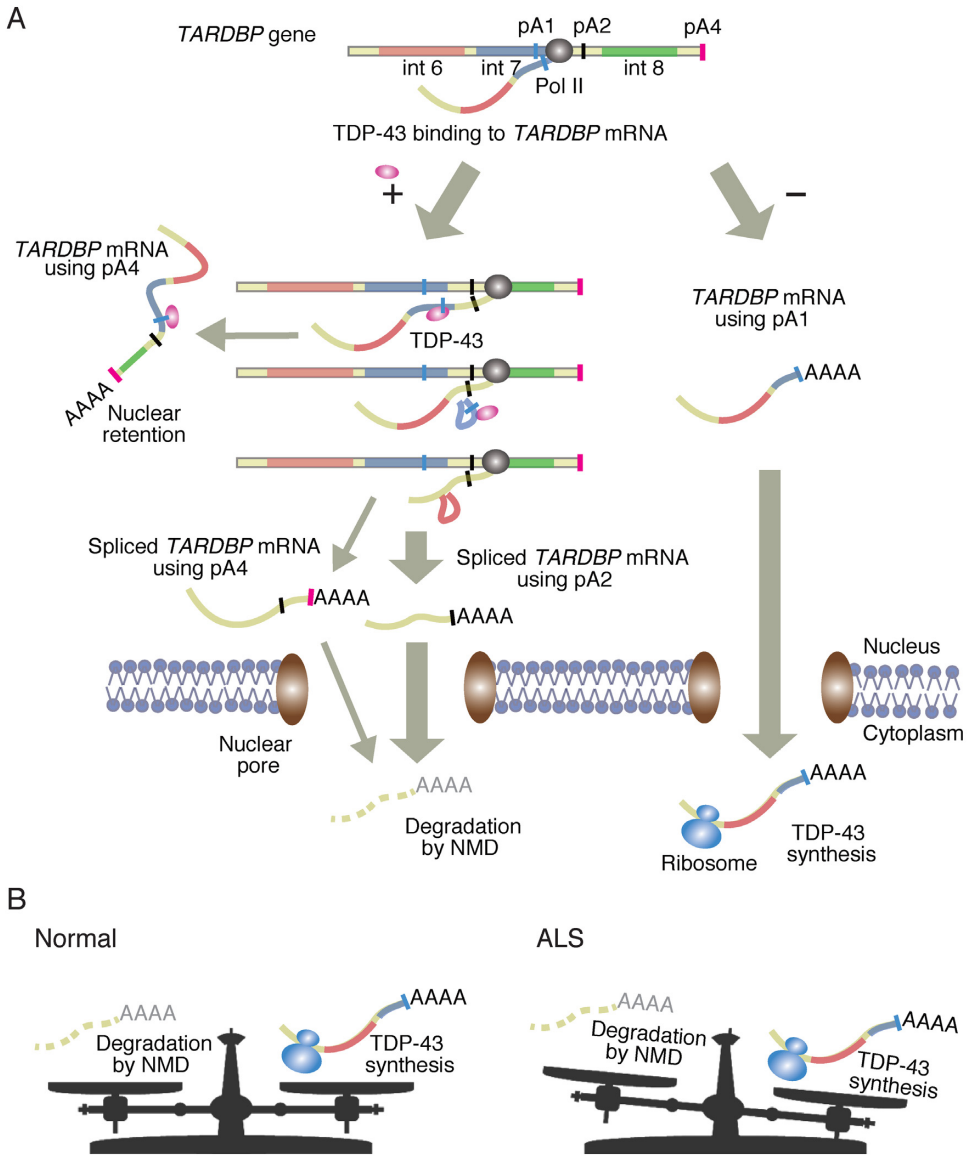

Figure 9. Autoregulation model of TDP-43. (**A**) The fate of *TARDBP* mRNA (curved lines) is determined by TDP-43 (red ovals). With an excess amount of nuclear TDP-43, TDP-43 binds to intron 7 of *TARDBP* mRNA and inhibits the selection of pA1 located in intron 7 (int 7: blue boxes and lines) (left stream). Then, the transcripts extending beyond pA1 present the acceptor site of intron 7. Most of the transcripts undergo the splicing of intron 7, followed by the splicing of intron 6 (int 6: orange boxes and lines). This spliced mRNA uses pA2 (black vertical lines) or pA4 (pink vertical lines) and is exported to the cytoplasm and degraded by a nonsense-mediated mRNA decay mechanism. A small number of transcripts using pA4 escaped this fate but was retained in nucleus. *TARDBP* mRNA, which is free from TDP-43, uses pA1 (pA1: blue vertical lines) and is transported to the cytoplasm, where it is then translated into TDP-43 (right stream). The curved lines represent a part of *TARDBP* pre-mRNA and mRNA. The boxes represent a part of the *TARDBP* gene. The green boxes and lines represent intron 8 (int 8). pA: polyadenylation signal; gray ovals: polymerase II (Pol II); light blue ovals: ribosome. (**B**) Schematic for *TARDBP* mRNA metabolism in healthy and ALS patients. In normal conditions, the production of TDP-43 is regulated by balancing between the transcription of splicing variants degraded by nonsense-mediated mRNA decay (left) and those that are translated (right). In ALS, this balance is shifted to produce transcripts that are translated.

Their probes could not detect the isoforms that contribute to autoregulation because intron 7 is excised when TDP-43 is downregulated, and intron 6 shows marked diversity. Second, we used poly(A)$^+$ RNA from the cytoplasmic or nuclear fraction to increase sensitivity, whereas they used total RNA from whole cell extracts. Moreover, instead, based on results from experiments with minigenes containing a part of *TARDBP*, they proposed that an isoform lacking only intron 7 is retained in the nucleus (5,7). However, we found that the isoform lacking only intron 7 is not a major isoform in the nucleus and cytoplasm (Figure 1D and F).

We have shown the importance of splicing intron 6 for the autoregulation of TDP-43. Although the splicing of intron 7 fulfills the criteria for nonsense-mediated mRNA decay, both introns were spliced out in most transcripts degraded by a nonsense-mediated mRNA decay pathway. The mutated minigene analysis revealed that the splicing of intron 7 is important for the splicing of intron 6 and not just for

binding TDP-43. Moreover, inhibiting the splicing of intron 6 resulted in a smaller decrease in the amount of protein product derived from the *TARDBP* exon 6-fused minigene after ectopic TDP-43 expression. Interestingly, the mutations observed in ALS10 patients cluster within intron 6 (34). We found an increased amount of *TARDBP* mRNA in spinal motor neurons in ALS10 patients. In addition, an increased amount of *TARDBP* mRNA has been reported in iPS-derived neurons of ALS10 patients (35). Therefore, it would be interesting to investigate how the mutations observed in ALS10 patients affect the splicing of introns 6 and 7.

We demonstrated that TDP-43 is autoregulated by the amount of cytoplasmic *TARDBP* mRNA. The process is regulated by coordination between the use of different PASs and alternative splicing of *TARDBP* mRNA, accompanied by nonsense-mediated mRNA decay. Our observations demonstrate a role for nuclear TDP-43 in TDP-43 autoregulation and indicate that once the mislocalization of TDP-43 occurs, TDP-43 synthesis is upregulated by an autoregulatory mechanism in affected motor neurons in ALS patients. The vicious cycle might accelerate disease progression by inducing the formation of cytoplasmic inclusions (10–12) and/or the dysregulation of RNA metabolism (8,13–16). Breaking the vicious cycle of TDP-43 production by modulating the autoregulatory mechanism might provide a new therapeutic strategy for halting the progression of ALS.

SUPPLEMENTARY DATA

Supplementary Data are available at NAR Online.

FUNDING

Grant-in-aid for Scientific Research on Innovative Areas (Brain Protein Aging and Dementia Control) [26117006], Foundation of Synapse and Neurocircuit Pathology [25110714]; MEXT; Grants-in-aid for Scientific Research [26250017, 25253065]; Grant-in-aid for Young Scientists [15K19479] (Japan Society for the Promotion of Science); Grant-in-aid from the Research Committee of CNS Degenerative Diseases and Comprehensive Research on Disability, Health, and Welfare from the Japanese Ministry of Health, Labor, and Welfare, Japan [13230021]; Grant-in-aid from Takeda Science Foundation; Grant-in-aid from the Tsubaki Memorial Foundation; Grant-in-aid from JSPS Fellows from the Ministry of Education, Culture, Sports, Science, and Technology of Japan. Funding for open access charge: Scientific Research on Innovative Areas (Brain Protein Aging and Dementia Control) [26117006].
Conflict of interest statement. None declared.

REFERENCES

1. Arai,T., Hasegawa,M., Akiyama,H., Ikeda,K., Nonaka,T., Mori,H., Mann,D., Tsuchiya,K., Yoshida,M., Hashizume,Y. *et al.* (2006) TDP-43 is a component of ubiquitin-positive tau-negative inclusions in frontotemporal lobar degeneration and amyotrophic lateral sclerosis. *Biochem. Biophys. Res. Commun.*, **351**, 602–611.
2. Lee,E.B., Lee,V.M. and Trojanowski,J.Q. (2012) Gains or losses: molecular mechanisms of TDP43-mediated neurodegeneration. *Nat. Rev. Neurosci.*, **13**, 38–50.
3. Neumann,M., Sampathu,D.M., Kwong,L.K., Truax,A.C., Micsenyi,M.C., Chou,T.T., Bruce,J., Schuck,T., Grossman,M., Clark,C.M. *et al.* (2006) Ubiquitinated TDP-43 in frontotemporal lobar degeneration and amyotrophic lateral sclerosis. *Science*, **314**, 130–133.
4. Tan,C.F., Eguchi,H., Tagawa,A., Onodera,O., Iwasaki,T., Tsujino,A., Nishizawa,M., Kakita,A. and Takahashi,H. (2007) TDP-43 immunoreactivity in neuronal inclusions in familial amyotrophic lateral sclerosis with or without SOD1 gene mutation. *Acta Neuropathol.*, **113**, 535–542.
5. Avendano-Vazquez,S.E., Dhir,A., Bembich,S., Buratti,E., Proudfoot,N. and Baralle,F.E. (2012) Autoregulation of TDP-43 mRNA levels involves interplay between transcription, splicing, and alternative polyA site selection. *Genes Dev.*, **26**, 1679–1684.
6. Ayala,Y.M., De Conti,L., Avendano-Vazquez,S.E., Dhir,A., Romano,M., D'Ambrogio,A., Tollervey,J., Ule,J., Baralle,M., Buratti,E. *et al.* (2011) TDP-43 regulates its mRNA levels through a negative feedback loop. *EMBO J.*, **30**, 277–288.
7. Bembich,S., Herzog,J.S., De Conti,L., Stuani,C., Avendano-Vazquez,S.E., Buratti,E., Baralle,M. and Baralle,F.E. (2014) Predominance of spliceosomal complex formation over polyadenylation site selection in TDP-43 autoregulation. *Nucleic Acids Res.*, **42**, 3362–3371.
8. Polymenidou,M., Lagier-Tourenne,C., Hutt,K.R., Huelga,S.C., Moran,J., Liang,T.Y., Ling,S.C., Sun,E., Wancewicz,E., Mazur,C. *et al.* (2011) Long pre-mRNA depletion and RNA missplicing contribute to neuronal vulnerability from loss of TDP-43. *Nat. Neurosci.*, **14**, 459–468.
9. Budini,M. and Buratti,E. (2011) TDP-43 autoregulation: implications for disease. *J. Mol. Neurosci.*, **45**, 473–479.
10. Swarup,V., Phaneuf,D., Dupre,N., Petri,S., Strong,M., Kriz,J. and Julien,J.P. (2011) Deregulation of TDP-43 in amyotrophic lateral sclerosis triggers nuclear factor kappaB-mediated pathogenic pathways. *J. Exp. Med.*, **208**, 2429–2447.
11. Tsao,W., Jeong,Y.H., Lin,S., Ling,J., Price,D.L., Chiang,P.M. and Wong,P.C. (2012) Rodent models of TDP-43: recent advances. *Brain Res.*, **1462**, 26–39.
12. Wils,H., Kleinberger,G., Janssens,J., Pereson,S., Joris,G., Cuijt,I., Smits,V., Ceuterick-de Groote,C., Van Broeckhoven,C. and Kumar-Singh,S. (2010) TDP-43 transgenic mice develop spastic paralysis and neuronal inclusions characteristic of ALS and frontotemporal lobar degeneration. *Proc. Natl. Acad. Sci. U.S.A.*, **107**, 3858–3863.
13. Lagier-Tourenne,C., Polymenidou,M., Hutt,K.R., Vu,A.Q., Baughn,M., Huelga,S.C., Clutario,K.M., Ling,S.C., Liang,T.Y., Mazur,C. *et al.* (2012) Divergent roles of ALS-linked proteins FUS/TLS and TDP-43 intersect in processing long pre-mRNAs. *Nat. Neurosci.*, **15**, 1488–1497.
14. Shiga,A., Ishihara,T., Miyashita,A., Kuwabara,M., Kato,T., Watanabe,N., Yamahira,A., Kondo,C., Yokoseki,A., Takahashi,M. *et al.* (2012) Alteration of POLDIP3 splicing associated with loss of function of TDP-43 in tissues affected with ALS. *PLoS One*, **7**, e43120.
15. Tollervey,J.R., Curk,T., Rogelj,B., Briese,M., Cereda,M., Kayikci,M., Konig,J., Hortobagyi,T., Nishimura,A.L., Zupunski,V. *et al.* (2011) Characterizing the RNA targets and position-dependent splicing regulation by TDP-43. *Nat. Neurosci.*, **14**, 452–458.
16. Ling,J.P., Pletnikova,O., Troncoso,J.C. and Wong,P.C. (2015) NEURODEGENERATION. TDP-43 repression of nonconserved cryptic exons is compromised in ALS-FTD. *Science*, **349**, 650–655.
17. Kraemer,B.C., Schuck,T., Wheeler,J.M., Robinson,L.C., Trojanowski,J.Q., Lee,V.M. and Schellenberg,G.D. (2010) Loss of murine TDP-43 disrupts motor function and plays an essential role in embryogenesis. *Acta Neuropathol.*, **119**, 409–419.
18. Yokoseki,A., Shiga,A., Tan,C.F., Tagawa,A., Kaneko,H., Koyama,A., Eguchi,H., Tsujino,A., Ikeuchi,T., Kakita,A. *et al.* (2008) TDP-43 mutation in familial amyotrophic lateral sclerosis. *Ann. Neurol.*, **63**, 538–542.
19. Wang,H.Y., Wang,I.F., Bose,J. and Shen,C.K. (2004) Structural diversity and functional implications of the eukaryotic TDP gene family. *Genomics*, **83**, 130–139.
20. Sun,S., Zhang,Z., Sinha,R., Karni,R. and Krainer,A.R. (2010) SF2/ASF autoregulation involves multiple layers of

post-transcriptional and translational control. *Nat. Struct. Mol. Biol.*, **17**, 306–312.
21. Jenal,M., Elkon,R., Loayza-Puch,F., van Haaften,G., Kuhn,U., Menzies,F.M., Oude Vrielink,J.A., Bos,A.J., Drost,J., Rooijers,K. *et al.* (2012) The poly(A)-binding protein nuclear 1 suppresses alternative cleavage and polyadenylation sites. *Cell*, **149**, 538–553.
22. McGlincy,N.J. and Smith,C.W. (2008) Alternative splicing resulting in nonsense-mediated mRNA decay: what is the meaning of nonsense? *Trends Biochem. Sci.*, **33**, 385–393.
23. Keeling,K.M., Wang,D., Dai,Y., Murugesan,S., Chenna,B., Clark,J., Belakhov,V., Kandasamy,J., Velu,S.E., Baasov,T. *et al.* (2013) Attenuation of nonsense-mediated mRNA decay enhances in vivo nonsense suppression. *PLoS One*, **8**, e60478.
24. Battich,N., Stoeger,T. and Pelkmans,L. (2013) Image-based transcriptomics in thousands of single human cells at single-molecule resolution. *Nat. Methods*, **10**, 1127–1133.
25. Schoenberg,D.R. and Maquat,L.E. (2012) Regulation of cytoplasmic mRNA decay. *Nat. Rev. Genet.*, **13**, 246–259.
26. Al-Ahmadi,W., Al-Ghamdi,M., Al-Haj,L., Al-Saif,M. and Khabar,K.S. (2009) Alternative polyadenylation variants of the RNA binding protein, HuR: abundance, role of AU-rich elements and auto-Regulation. *Nucleic Acids Res.*, **37**, 3612–3624.
27. Rabin,S.J., Kim,J.M., Baughn,M., Libby,R.T., Kim,Y.J., Fan,Y., Libby,R.T., La Spada,A., Stone,B. and Ravits,J. (2010) Sporadic ALS has compartment-specific aberrant exon splicing and altered cell-matrix adhesion biology. *Hum. Mol. Genet.*, **19**, 313–328.
28. Takahashi,H., Makifuchi,T., Nakano,R., Sato,S., Inuzuka,T., Sakimura,K., Mishina,M., Honma,Y., Tsuji,S. and Ikuta,F. (1994) Familial amyotrophic lateral sclerosis with a mutation in the Cu/Zn superoxide dismutase gene. *Acta Neuropathol.*, **88**, 185–188.
29. Tan,C.F., Piao,Y.S., Hayashi,S., Obata,H., Umeda,Y., Sato,M., Fukushima,T., Nakano,R., Tsuji,S. and Takahashi,H. (2004) Familial amyotrophic lateral sclerosis with bulbar onset and a novel Asp101Tyr Cu/Zn superoxide dismutase gene mutation. *Acta Neuropathol.*, **108**, 332–336.
30. Oyanagi,K., Ikuta,F. and Horikawa,Y. (1989) Evidence for sequential degeneration of the neurons in the intermediate zone of the spinal cord in amyotrophic lateral sclerosis: a topographic and quantitative investigation. *Acta Neuropathol.*, **77**, 343–349.
31. Lareau,L.F., Inada,M., Green,R.E., Wengrod,J.C. and Brenner,S.E. (2007) Unproductive splicing of SR genes associated with highly conserved and ultraconserved DNA elements. *Nature*, **446**, 926–929.
32. Ni,J.Z., Grate,L., Donohue,J.P., Preston,C., Nobida,N., O'Brien,G., Shiue,L., Clark,T.A., Blume,J.E. and Ares,M. Jr (2007) Ultraconserved elements are associated with homeostatic control of splicing regulators by alternative splicing and nonsense-mediated decay. *Genes Dev.*, **21**, 708–718.
33. Romero,P.R., Zaidi,S., Fang,Y.Y., Uversky,V.N., Radivojac,P., Oldfield,C.J., Cortese,M.S., Sickmeier,M., LeGall,T., Obradovic,Z. *et al.* (2006) Alternative splicing in concert with protein intrinsic disorder enables increased functional diversity in multicellular organisms. *Proc. Natl. Acad. Sci. U.S.A.*, **103**, 8390–8395.
34. Onodera,O., Sugai,A., Konno,T., Tada,M., Koyama,A. and Nishizawa,M. (2013) What is the key player in TDP-43 pathology in ALS: disappearance from the nucleus or inclusion formation in the cytoplasm? *Neurol. Clin. Neurosci.*, **1**, 11–17.
35. Egawa,N., Kitaoka,S., Tsukita,K., Naitoh,M., Takahashi,K., Yamamoto,T., Adachi,F., Kondo,T., Okita,K., Asaka,I. *et al.* (2012) Drug screening for ALS using patient-specific induced pluripotent stem cells. *Sci. Transl. Med.*, **4**, 145ra104.